TOPICAL REVIEW

Multiphonon giant resonances

C A Bertulani†

Instituto de Física, Universidade Federal do Rio de Janeiro 21945-970, Rio de Janeiro, RJ, Brazil

Abstract. A new class of giant resonances in nuclei is discussed, i.e. giant resonances built on other giant resonances. These resonances are observed with very large cross sections in relativistic heavy ion collisions. A great experimental and theoretical effort is underway to understand the reaction mechanism which leads to the excitation of these states in nuclei, as well as the better microscopic understanding of their properties, for example, strength, energy centroids, widths and anharmonicities.

1. Giant Resonances

1.1. Single giant resonances

Giant resonances in nuclei were first observed in 1937 by Bothe and Gentner [1] who observed an unexpectedly large absorption of 17.6 MeV photons (from the ^{7}Li(p, γ) reaction) in some targets. These observations were later confirmed by Baldwin and Klaiber (1947) with photons from a betatron. In 1948 Goldhaber and Teller [2] interpreted these resonances (called isovector giant dipole resonances (IVGDR)) with a hydrodynamical model in which rigid proton and neutron fluids vibrate against each other, the restoring force resulting from the surface energy. Steinwendel and Jensen [3] later developed the model, considering compressible neutron and proton fluids vibrating in opposite phase in a common fixed sphere, the restoring force resulting from the volume symmetry energy. The standard microscopic basis for the description of giant resonances is the random phase approximation (RPA) in which giant resonances appear as coherent superpositions of one-particle one-hole ($1p1h$) excitations in closed shell nuclei or two quasiparticle excitations in open shell nuclei (for a review of these techniques, see, for example, [4]).

The isoscalar quadrupole resonances were discovered in inelastic electron scattering by Pitthan and Walcher (1971) and in proton scattering by Lewis and Bertrand (1972). Giant monopole resonances were found later and their properties are closely related to the compression modulus of nuclear matter. Following these, other resonances of higher multipolarities and giant magnetic resonances were investigated. Typical probes for giant resonance studies are (a) γ's and electrons for the excitation of IVGDR, (b) α-particles and electrons for the excitation of isoscalar giant monopole resonance (ISGMR) and giant quadrupole resonance (ISGQR), and (c) (p, n), or (^{3}He, t), for Gamow–Teller resonances, respectively.
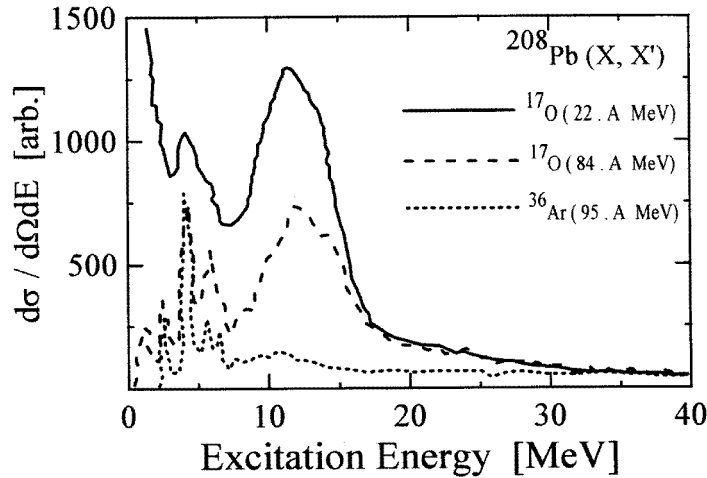
† E-mail address: bertu@if.ufrj.br

Figure 1. Experimental cross sections in arbitrary units for the excitation of ^{208}Pb targets by ^{17}O (22A MeV and 84A MeV) and by ^{36}Ar (95A MeV), as a function of the excitation energy.

1.2. Multiphonon resonances

Inelastic scattering studies with heavy ion beams have opened new possibilities in the field (for a review of the experimental developments, see [5]). A striking feature was observed when either the beam energy was increased, or heavier projectiles were used, or both [6]. This is displayed in figure 1, where the excitation of the GDR in ^{208}Pb was observed in the inelastic scattering of ^{17}O at 22 MeV/nucleon and 84 MeV/nucleon, respectively, and ^{36}Ar at 95 MeV/nucleon [7, 8]. What one clearly sees is that the 'bump' corresponding to the GDR at 13.5 MeV is appreciably enhanced. This feature is solely due to one agent: the electromagnetic interaction between the nuclei. This interaction is more effective at higher energies, and for increasing charge of the projectile.

In [9] it was noted that the excitation probabilities of the GDR in heavy ion collisions approach unity at grazing impact parameters. It was further shown that, if DGDR (double GDR) (i.e. a GDR excited on a GDR state) exists then the cross sections for their excitation in heavy ion collisions at relativistic energies are of the order of hundreds of millibarns. This calculation was based on the semiclassical approach, appropriate for heavy ion scattering at high incident energies, and the harmonic oscillator model for the giant resonances. The semiclassical model treats the relative motion between the nuclei classically while quantum mechanics is used for the internal degrees of freedom.

In the harmonic picture for the internal degrees of freedom the GDR is the first excited state in a harmonic well, the GDR^2, or DGDR, is the second state, and so on. In [10] it was shown that the excitation probabilities and cross sections are directly proportional to the photonuclear cross sections for a given electric (E) and magnetic (M) multipolarity. For an impact parameter b, excitation energy E, and a multipolarity $\pi\lambda$ ($\pi = E$ or M) the excitation probabilities are given by

$$P_{\pi\lambda}(E, b) = \frac{1}{E} N_{\pi\lambda}(E, b) \sigma_\gamma^{\pi\lambda}(E) \tag{1}$$

where $\sigma_\gamma^{\pi\lambda}(E)$ is the photonuclear cross sections for the photon E and multipolarity $\pi\lambda$. The total photonuclear cross section is $\sigma_\gamma(E) = \sum_{\pi\lambda} \sigma_\gamma^{\pi\lambda}(E)$. In the semiclassical approach,

the 'equivalent photon numbers' $N_{\pi\lambda}(E, b)$ are given analytically [10]. A quantum mechanical derivation of the excitation amplitudes in relativistic Coulomb excitation shows that equation (1) can also be obtained by using the saddle-point approximation in the distorted wave Born approximation (DWBA) integrals [11]. The total Coulomb excitation cross sections can be obtained by an integration of equation (1) over the impact parameter b, including a factor, $T(b)$, which accounts for the strong absorption at small impact parameters: $\sigma_{\pi\lambda}(E) = 2\pi \int \mathrm{d}b\, bT(b) P_{\pi\lambda}(E, b)$. The impact parameter integral can also be performed analytically and the equivalent photon numbers $n_{\pi\lambda}(E) = 2\pi \int \mathrm{d}b\, bN_{\pi\lambda}(E, b)$ are given in [10, 11].

The cross section for the excitation of a giant resonance is obtained from these expressions, by using the experimental photonuclear absorption cross section for $\sigma_\gamma^{\pi\lambda}(E)$ in equation (1). One problem with this procedure is that the experimental photonuclear cross section includes all multipolarities with the same weight: $\sigma_\gamma^{\exp}(E) = \sum_{\pi\lambda} \sigma_\gamma^{\pi\lambda}(E)$, while the calculation based on equation (1) needs the isolation of $\sigma_\gamma^{\pi\lambda}(E)$. This can only be done marginally, except in some exclusive measurements. Generally, one finds in the literature the (γ, n), $(\gamma, 2\mathrm{n})$, and $(\gamma, 3\mathrm{n})$ cross sections, which include the contribution of all multipolarities in the giant resonance energy region. A separation of the different multipolarities can be obtained roughly by use of sum rules, or some theoretical model for the nuclear response to a photoexcitation.

Assuming that one has $\sigma_\gamma^{\pi\lambda}(E)$ somehow (either from experiments, or from theory), a simple harmonic model based on the Axel–Brink hypotheses can be formulated to obtain the probability to access a multiphonon state of order n. In the harmonic oscillator model the inclusion of the coupling between all multiphonon states can be performed analytically [9]. One of the basic changes is that the excitation probabilities are calculated to first-order, $P_{\pi\lambda}^{\mathrm{1st}}(E, b)$, are modified to include the flux of probability to the other states. That is,

$$P_{\pi\lambda}(E, b) = P_{\pi\lambda}^{\mathrm{1st}}(E, b) \exp\{-P_{\pi\lambda}^{\mathrm{1st}}(b)\} \tag{2}$$

where $P_{\pi\lambda}^{\mathrm{1st}}(b)$ is the integral over the excitation energy E. In general, the probability to reach a multiphonon state with the energy $E^{(n)}$ from the ground state, with energy $E^{(0)}$, is obtained by an integral over all intermediate energies

$$P_{\pi^*\lambda^*}^{(n)}(E^{(n)}, b) = \frac{1}{n!} \exp\{-P_{\pi\lambda}^{\mathrm{1st}}(b)\} \int \mathrm{d}E^{(n-1)}\, \mathrm{d}E^{(n-2)} \dots \mathrm{d}E^{(1)}$$
$$\times P_{\pi\lambda}^{\mathrm{1st}}(E^{(n)} - E^{(n-1)}, b) P_{\pi\lambda}^{\mathrm{1st}}(E^{(n-1)} - E^{(n-2)}, b) \dots P_{\pi\lambda}^{\mathrm{1st}}(E^{(1)} - E^{(0)}, b). \tag{3}$$

The character and spin assignment of the multipolarity λ^* depends on how the intermediate states couple with the electromagnetic transition operators. For example, in the case of the DGDR (GDR^2), assuming a 0^+ ground state and excluding isospin impurities, the final state has either spin and parity 0^+ or 2^+, respectively.

A simpler reaction model than the one above can be obtained when assuming that all states can be approximated by a single isolated state. For example, we can assume that the photoabsorption cross sections in the range of the GDR is due to a single state with energy equal to the centroid energy of the GDR exhausting the whole excitation strength. Then the multiphonon states are equidistant, and equation (3) becomes

$$P_{\pi^*\lambda^*}^{(n)}(b) = \frac{1}{n!} [P_{\pi\lambda}^{\mathrm{1st}}(b)]^n \exp\{-P_{\pi\lambda}^{\mathrm{1st}}(b)\}. \tag{4}$$

The above relation was used to calculate the cross sections for the excitation of the GDR, GDR^2, GDR^3, ISGQR and IVGQR in ^{136}Xe, respectively, for collisions with Pb nuclei as a function of the bombarding energy, as shown in figure 2. Each resonance is considered to be a single state exhausting 100% of the respective sum rule. Also shown in the figure
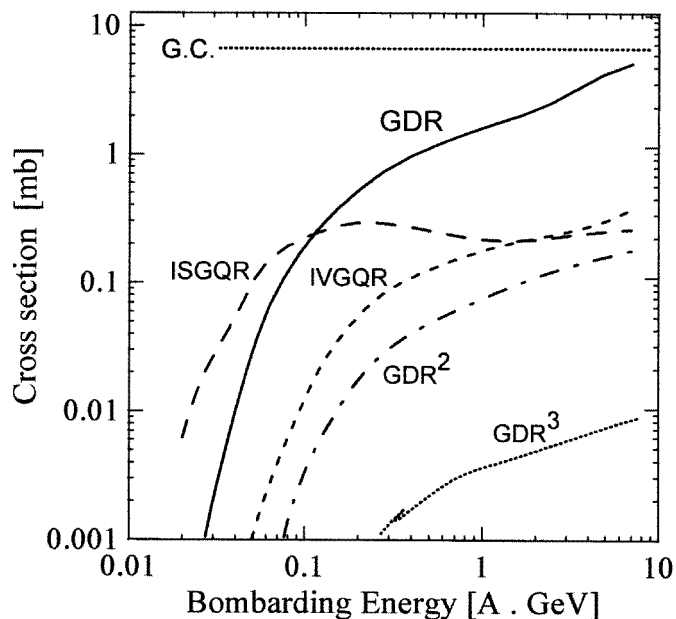
Figure 2. Theoretical cross sections for the excitation of the GDR, ISGQR, IVGQR, GDR^2 and the GDR^3, in the reaction ^{208}Pb $+$ ^{208}Pb, as a function of the bombarding energy.

is the geometrical cross section (GC), $\sigma \sim \pi(A_P^{1/3} + A_T^{1/3})^2$ fm^2. The cross sections for the excitation of the GDR^2 is large, of the order of hundreds of mb.

Much of the interest in looking for multiphonon resonances relies on the possibility for looking at exotic particle decay of these states. For example, in [15] a hydrodynamical model was used to predict the proton and neutron dynamical densities in a multiphonon state of a nucleus. Large proton and neutron excesses at the surface are developed in a multiphonon state. Thus, the emission of exotic clusters from the decay of these states are a natural possibility. A more classical point of view is that the Lorentz contracted Coulomb field in a peripheral relativistic heavy ion collision acts as a hammer on the protons of the nuclei [10]. This (collective) motion of the protons seems only to be probed in relativistic Coulomb excitation. It is not well known how this classical view can be related to microscopic properties of the nuclei in a multiphonon state.

Although the perspectives for experimental evidence of the DGDR via relativistic Coulomb excitation were good, on the basis of the large theoretical cross sections, it was first found in pion scattering at the Los Alamos Pion Facility [12]. In pion scattering off nuclei the DGDR can be described as a two-step mechanism induced by the pion–nucleus interaction. Using the Axel–Brink hypotheses, the cross sections for the excitation of the DGDR with pions were shown to be well within the experimental possibilities [12]. Only about five years later, the first Coulomb excitation experiments for the excitation of the DGDR were performed at the GSI facility in Darmstadt/Germany [13, 14]. In figure 3 we show the result of one of these experiments, which looked for the neutron decay channels of giant resonances excited in relativistic projectiles. The excitation spectrum of relativistic ^{136}Xe projectiles incident on Pb are compared with the spectrum obtained in C targets. A comparison of the two spectra immediately proves that nuclear contribution to the excitation is very small. Another experiment [14] dealt with the photon decay of the double giant
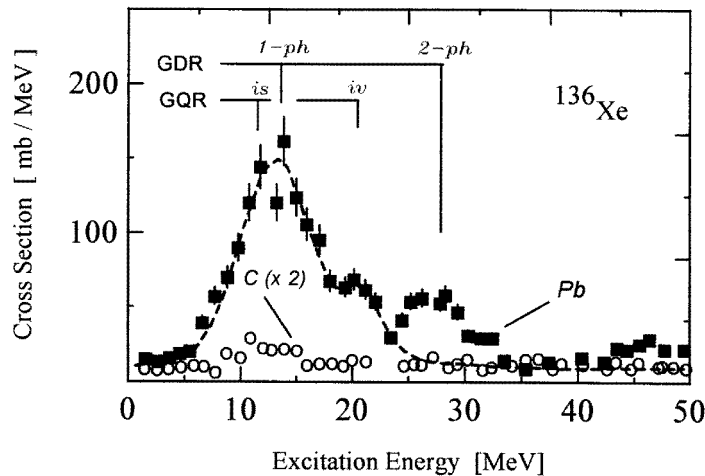
Figure 3. Experimental cross sections for the excitation of ^{136}Xe ($700A$ MeV) projectiles incident on lead and carbon targets, respectively.

resonance. A clear bump in the spectra of coincident photon pairs was observed around an energy twice as large as the GDR centroid energy in ^{208}Pb targets excited with relativistic ^{209}Bi projectiles.

The advantages of relativistic Coulomb excitation of heavy ions over other probes (pions, nuclear excitation, etc) was clearly demonstrated in several GSI experiments [13, 14, 16, 17]. We now discuss many features of the DGDR that were obtained.

2. Energy, width and strength of the DGDR

A collection of the experimental data on the energy and width of the DGDR is shown in figure 4. The data points are from a compilation from pion (open symbols), and Coulomb excitation and nuclear excitation (full symbols) experiments [18].

The broken curves are a guide for the eyes. We see from figure 4(*a*) that the energy of the DGDR agrees reasonably with the expected harmonic prediction that the energy should be about twice the energy of the GDR, although small departures from this prediction are seen, especially in pion and nuclear excitation experiments. The width of the DGDR seems to agree with an average value of $\sqrt{2}$ times that of the GDR, although a factor of 2 seems also to be possible, as we see from figure 4(*b*). Figure 4(*c*) shows the ratio between the experimentally determined cross sections and the calculated ones. The data appear to be more dispersed here. The largest values of $\sigma_{\text{exp}}/\sigma_{\text{th}}$ come from pion experiments, yielding up to a value of 5 for this quantity.

2.1. Width of the DGDR

In a microscopic approach, the GDR is described by a coherent superposition of one-particle one-hole states. One of the many such states is pushed up by the residual interaction to the experimentally observed position of the GDR. This state carries practically all of the $E1$ strength. This situation is simply realized in a model with a separable residual interaction. We write the GDR state as (one phonon with angular momentum $1M$)$|1, 1M\rangle = A^{\dagger}_{1M}|0\rangle$
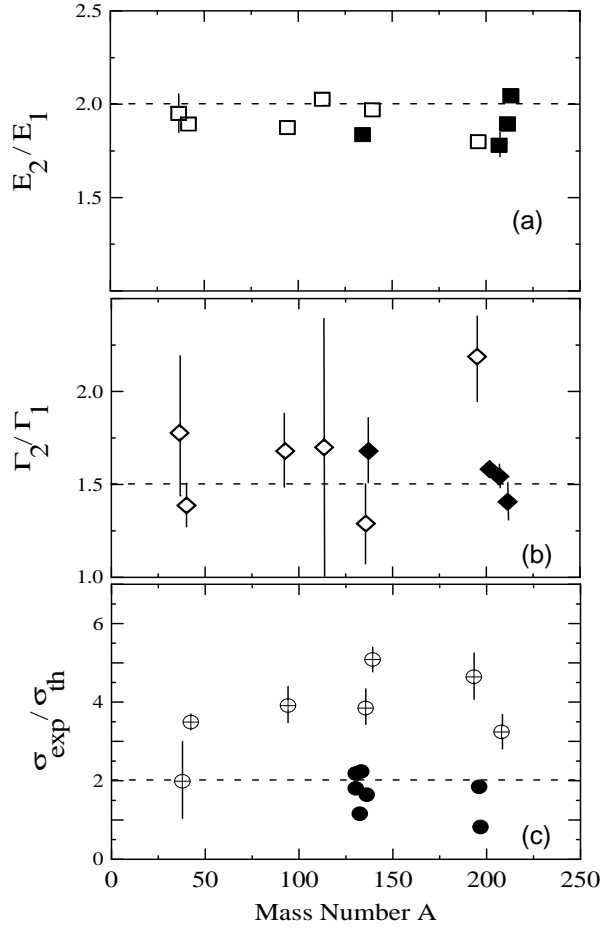
Figure 4. Compilation of experimental findings with heavy ion (full symbols) and pion induced (open symbols) reactions for the energy, width, and cross sections of the double giant resonance. The data are compared with the energies and widths of the GDR, respectively, and to the theoretical excitation cross sections.

where $A^{\dagger}_{1M}$ is a proper superposition of particle–hole creation operators. Applying the quasiboson approximation we can use the boson commutation relations and construct the multiphonon states (N-phonon states). An N-phonon state will be a coherent superposition of N-particle N-hole states. The width of the GDR is essentially due to the spreading width, i.e. to the coupling to more complicated quasibound configurations. The escape width only plays a minor role. We are not interested in a detailed microscopic description of these states here. We use a simple model for the strength function [19]. We couple a state $|a\rangle$ (i.e. a GDR state) by some mechanism to more complicated states $|\alpha\rangle$, for simplicity we assume a constant coupling matrix element $V_{a\alpha} = \langle a|V|\alpha\rangle = \langle\alpha|V|a\rangle = v$. With an equal spacing of D of the levels $|\alpha\rangle$ one obtains a width

$$\Gamma = 2\pi \frac{v^2}{D} \tag{5}$$

for the state $|\alpha\rangle$. We assume the same mechanism to be responsible for the width of the N-phonon state: one of the N-independent phonons decays into the more complicated states

$|\alpha\rangle$ while the other $(N-1)$-phonons remain spectators. We write the coupling interaction in terms of creation (destruction) operators $c_a^\dagger(c_\alpha)$ of the complicated states $|\alpha\rangle$ as

$$V = v(A_{1M}^\dagger c_\alpha + A_{1M} c_\alpha^\dagger). \tag{6}$$

For the coupling matrix elements v_N, which connects an N-phonon state $|N\rangle$ to the state $|N-1,\alpha\rangle$ $(N-1$ spectator phonons) one obtains

$$v_N = \langle N-1,\alpha|V|N\rangle = v\langle N-1|A_{1M}|N\rangle = v \cdot \sqrt{N} \tag{7}$$

i.e. one obtains for the width Γ_N of the N-phonon state

$$\Gamma = 2\pi N \frac{v^2}{D} = N\Gamma \tag{8}$$

where Γ is given by equation (5).

Thus, the factor N in (8) arises naturally from the bosonic character of the collective states. For the DGDR this would mean $\Gamma_2 = 2\Gamma_1$. The data points shown in figure 4(b) seem to favour a lower multiplicative factor.

We can also give a qualitative explanation for a smaller Γ_2/Γ_1 value. First we note that the value $\Gamma_2/\Gamma_1 = N$ can also be obtained from a folding procedure, as given in equation (3). If the sequential excitations are described by Breit–Wigner (BW) functions $P_{\pi\lambda}(E)$ with the centroid $\mathcal{E}$ and the width Γ, the convolution (3) yields a BW shape with the centroid at $2\mathcal{E}$ for the DGDR and the total width of $2\Gamma_1$. However, if one uses Gaussian functions (instead of BW ones) for the shape of one-phonon states, it is easy to show that one also obtains a Gaussian for the N-phonon shape, but with the width given by $\sqrt{N}\Gamma_1$. The latter assumption seems inconsistent since the experimentalists use BW fits for the shape of giant resonances, which are in good agreement with the experimental data. However, one can easily understand that the result $\sqrt{N}\Gamma_1$ is not restricted to a Gaussian fit. For an arbitrary sequence of two excitation processes we have $\langle E\rangle = \langle E_1 + E_2\rangle$ and $\langle E^2\rangle = \langle(E_1 + E_2)^2\rangle$; for uncorrelated steps it results in the addition in quadrature $(\Delta E)^2 = (\Delta E_1)^2 + (\Delta E_2)^2$. Identifying these fluctuations with the widths up to a common factor, we obtain for identical phonons $\Gamma_2 = \sqrt{2}\Gamma_1$. The same conclusion will be valid for any distribution function which, as the Gaussian one has a finite second moment, in contrast to the BW or Lorentzian ones with second moment diverging. We may conclude that, in physical terms, the difference between $\Gamma_2/\Gamma_1 = 2$ and $\Gamma_2/\Gamma_1 = \sqrt{2}$ is due to the different treatment of the wings of the distribution functions which reflect small admixtures of remote states.

2.2. Strength of the DGDR

Microscopically, the harmonic picture is accomplished within the RPA approximation. The excited states of the nucleus are described as superpositions of particle–hole configurations with respect to the ground state. The multiphonon resonances are built using products of the 1^- resonance states, yielding 0^+ and 2^+ double phonon states. The interaction with the projectile is described in terms of a linear combination of particle–hole operators weighted by the time-dependent field for a given multipolarity of the interaction. Since the time-dependent Coulomb field of a nucleus does not carry monopole multipolarity, the DGDR states can be reached via two-step $E1$ transitions and direct $E2$ transitions (for a 0^+ ground state). As we see from figure 4(c), early calculations failed to explain the experimental data. Owing to the simpler excitation mechanism we restrict ourselves to the Coulomb excitation cross sections. Then, there seems to be two possible reasons for $\sigma_{\rm exp}/\sigma_{\rm th} \neq 1$; (a) either the Coulomb excitation mechanism is not well described, or (b) the response of the nucleus to two-phonon excitations is not well known.

Many authors studied the effects of the excitation mechanism for the excitation of the DGDR. In [20] the cross sections were calculated using second-order perturbation theory. It was found that the theoretical values were smaller than the experimental ones by a factor of about 1.3–2. However, it was suggested [21] that second-order perturbation theory is not adequate for relativistic Coulomb excitation of giant resonances with heavy ions and that it is necessary to perform a coupled channels calculation. We can see this more clearly from figure 5, taken from [22], where a coupled-channels study of multiphonon excitation by the nuclear and Coulomb excitations in relativistic heavy ion collisions was performed. The figure shows the probability amplitude to excite the GDR in ^{208}Pb, $|a_1|^2$, and the occupation probability of the ground state, $|a_0|^2$, for a grazing collision of ^{208}Pb $+$ ^{208}Pb at 640 MeV/nucleon. The broken curves are the predictions of the first-order perturbation theory. We see that the asymptotic excitation probability of the GDR is quite large ($\sim$40%). In first-order perturbation the occupation probability of the ground state is kept constant, equal to unity. Obviously, one greatly violates the unitarity condition in this case. A more appropriate coupled-channels calculation (full curves) shows that the ground-state occupation probability has to decrease to meet the unitarity requirements, while the excitation probability of the GDR is also reduced slightly for the same reason.

In [22] it was shown that a good coupled-channels calculation does not need to account for the exact coupling equations in all channels. The strongest coupling, responsible for the effect observed in figure 5 is the coupling between the ground state and the GDR states. This has to be treated exactly within a coupled-channels calculation. The coupling between the GDR and the other states (including the DGDR, IVGQR, ISGQR, etc) can be treated
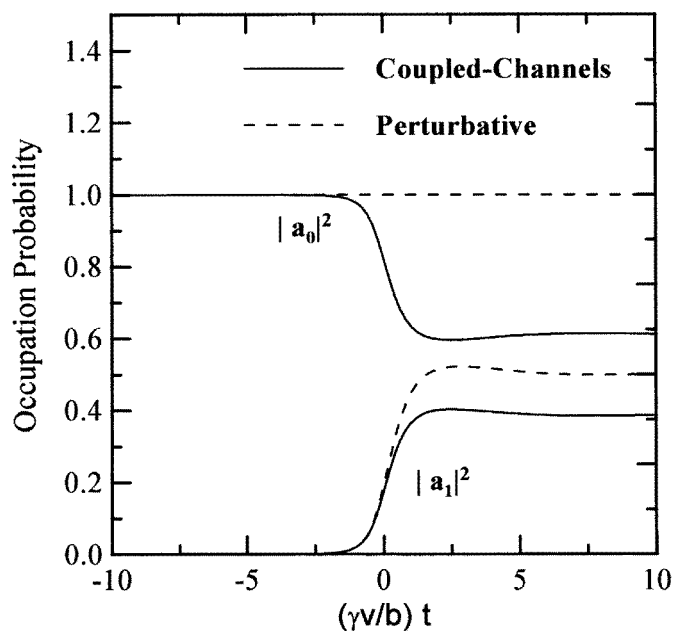

Figure 5. Occupation probability of the ground state, $|a_0|^2$, and of the GDR, $|a_1|^2$, for the reaction ^{208}Pb $+^{208}$ Pb at 640A MeV, as a function of the reaction time. The reaction time is given in terms of the adimensional quantity $\gamma v t/b$, with b equal to the impact parameter in the collision. The broken curves are the predictions of perturbation theory, while the full curves are the predictions from coupled-channels calculations.
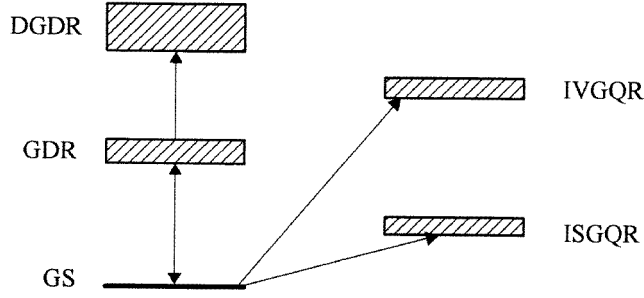
Figure 6. Schematic diagram showing the excitation of the GDR, ISGQR, IVGQR, and the DGDR. The arrow with two heads between the ground state GS and the GDR means that this coupling is to be treated exactly, i.e. with a coupled-channels calculation.

perturbatively, as shown schematically in figure 6. This amounts to a great simplification of the calculation. In fact, it allows us to include the width of the GDR in the coupled-channels calculation straightforwardly using a BW strength function for the GDR. In terms of the auxiliary amplitudes $A_\mu(t)$, given by the relation $a_0(t) = 1 + \sum_\mu A_\mu(t)$, with $\mu = -1, 0, 1$, the coupled-channels equations are given by

$$\ddot{A}_\mu(t) - \left[\frac{\dot{V}_\mu^{(01)}(t)}{V_\mu^{(01)}(t)} - \frac{i}{\hbar} \left(E_1 - i\frac{\Gamma_1}{2} \right) \right] \dot{A}_\mu(t) + \mathcal{S}_1 \frac{|V_\mu^{(01)}(t)|^2}{\hbar^2} \left[1 + \sum_{\mu'} A_{\mu'}(t) \right] = 0 \qquad (9)$$

where the factor $\mathcal{S}_1$ is $\mathcal{S}_1 = 1$ for the BW-shape and $\mathcal{S}_1 = 1 - i\Gamma_1/2E_1$ for Lorentzian-shape, and $V_\mu^{(01)}(t)$ is the time-dependent Coulomb interaction between the ground state and the magnetic component μ of the GDR. With initial conditions $A_\mu(t = -\infty) = 0$, the solution of the above coupled-channels equation can be used to calculate the excitation probability of the GDR state with energy $E_1 + \epsilon$, given by

$$i\hbar \dot{a}_{\epsilon,1\mu}^{(1)}(t) = [\alpha^{(1)}(\epsilon) V_\mu^{(01)}(t)]^* \exp\{i(E_1 + \epsilon)t/\hbar\} a_0(t). \qquad (10)$$

where $\alpha^{(1)}(\epsilon)$ is a BW or Lorentzian shape function, with centroid at E_1. After the calculation of the occupation probability of the ground state, $|a_0(\infty)|^2$, and the excitation probability of the GDR, $\sum_\mu \int |a_{\epsilon,1\mu}(\infty)|^2 \, d\epsilon$, it is straightforward to calculate the excitation probabilities of the DGDR and of other giant resonances using perturbation theory, as shown schematically in figure 6. Excitation cross sections are obtained by integration over impact parameters.

The results of [22] showed appreciable dependence of the excitation cross sections of the GDR^2 on the width of both the GDR and the DGDR as can be seen in figure 7 for $^{208}Pb + ^{208}Pb$ at 640 MeV/nucleon. The full curve shows the GDR cross section as a function of the width of the DGDR, keeping the ratio $\Gamma_{DGDR}/\Gamma_{GDR} = \sqrt{2}$. The broken curve is obtained by fixing the value of $\Gamma_{GDR} = 4$ MeV and varying the value of Γ_{DGDR}. The cross sections decrease with energy since an increase of the width enhances the doorway amplitude to higher energies where Coulomb excitation is weaker. Based on this figure, we may conclude that the data seem to favour a value of $\Gamma_{DGDR}/\Gamma_{GDR} \simeq \sqrt{2}$. Figure 8 shows the ratio $\sigma_{DGDR}/\sigma_{GDR}$ as a function of the bombarding energy. We observe that the most favourable energies for the measurement of the DGDR corresponds to the SIS energies at the GSI-Darmstadt facility.
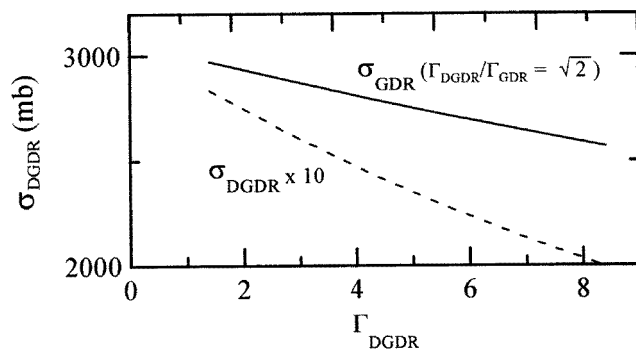
Figure 7. Cross section for the excitation of the GDR and the DGDR, as a function of the width of the GDR. The width of the DGDR is assumed to be $\sqrt{2}$ times the width of the GDR.
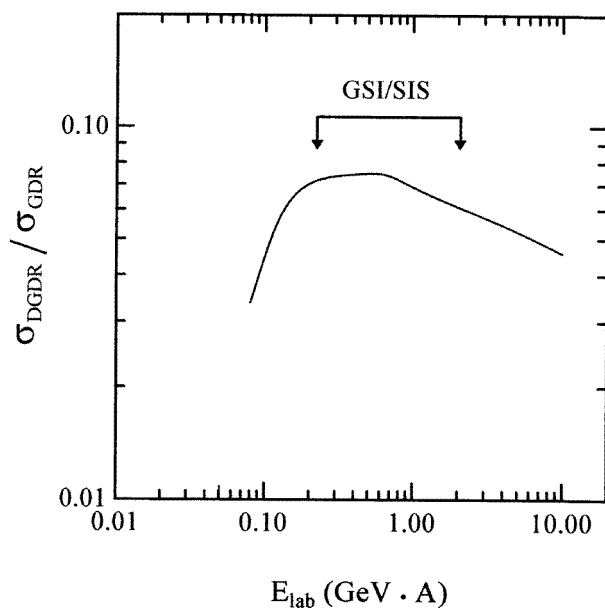

Figure 8. Ratio between the excitation cross sections of the DGDR and of the GDR for the reaction ^{208}Pb + ^{208}Pb, as a function of the bombarding energy. The arrows indicate the energy region of the GSI experiments.

2.3. Anharmonicities

Another possible effect arises from a shift of the energy centroid of the DGDR due to anharmonic effects [23]. In [22] one obtained $\sigma_{\text{DGDR}} = 620$, 299 and 199 mb for the centroid energies of $E_{\text{DGDR}} = 20$, 24 and 27 MeV, respectively. This shows that anharmonic effects can play a big role in the Coulomb excitation cross sections of the DGDR, depending on the size of the shift of E_{DGDR}. However, in [20] the source for anharmonic effects were discussed and it was suggested that it should be very small, i.e. $\Delta^{(2)} E = E_{\text{DGDR}} - 2E_{\text{GDR}} \simeq 0$.

The anharmonic behaviour of the giant resonances as a possibility to explain the increase of the Coulomb excitation cross sections has been studied by several authors [23, 24] (see

also [25], and references therein). It was found that the effect is indeed negligible and it could be estimated [25] as $\Delta^{(2)}E < E_{\text{GDR}}/(50\ A) \sim A^{-4/3}$ MeV.

2.4. Other routes to the DGDR

From the above discussion we see that the magnitude of the Coulomb excitation cross sections of the DGDR can be affected owing to uncertainties in: (a) strength, (b) width, (c) energies, or (d) reaction mechanism. Cases (a) and (c) are the basis of the Axel–Brink hypothesis and we have seen that a modification of their values would only be considered seriously if anharmonic effects were large, which appears not to be the case. Case (b) is an open question. Microscopic calculations [24] have shown that, taking into account the Landau damping, the collective state splits into a set of different 1_i^- states distributed over an energy interval, where i is the order number of each state. A further fragmentation of the 1_i^- states into thousands of closed packed states, is obtained by the coupling of one- and two-phonon states. This leads to a good estimate of the spreading width of the GDR. However, the DGDR states were obtained by a folding procedure:

$$|[1_i^- \otimes 1_{i'}^-]_{J^\pi = 0^+,1^+,2^+}\rangle_M = \sum_{m,m'} (1m1m'|JM)|1_i^-\rangle_m |1_{i'}^-\rangle_{m'}. \tag{11}$$

The width of the DGDR is thus fixed from the width of the GDR. Critics should be reminded that even the spreading width of the GDR is not very well described theoretically. It is therefore impossible to make any quantitative prediction for the width of the DGDR, other than saying that $\sqrt{2} \leqslant \Gamma_{\text{DGDR}}/\Gamma_{\text{GDR}} \leqslant 2$.

We return to the discussion of the reaction mechanism, and how it could affect the magnitude of the cross sections. It looks obvious from figure 3 that the nuclear excitation of giant resonances is very small in magnitude compared with Coulomb excitation in collisions with heavy ions at relativistic energies. However, the nuclear–Coulomb interference could also be relevant and would not be in complete disagreement with the experimental findings. However, in [22] it was shown that this is a small effect indeed.

We have seen that coupled-channels effects are very important and should always be considered in the analysis of the experimental results. In [26] the contribution of non-natural parity 1^+ two-phonon states were investigated in a coupled-channels calculation. The diagonal components $[1_i^- \otimes 1_i^-]_{1^+}$ are forbidden by symmetry properties but nondiagonal ones $[1_i^- \otimes 1_{i'}^-]_{1^+}$, *a priori*, may be excited in the two-step process bringing some 'extra strength' in the DGDR region. Consequently, the role of these nondiagonal components depends on how strong the Landau damping is.

The coupled-channels calculation found that the contribution of the 1^+ states to the total cross section is small. The reason for this is better explained in second-order perturbation theory. For any route to a final magnetic substate M, the second-order amplitude will be proportional to $(001\mu|1\mu)V_{E1\mu,0\to1^-} \times (1\mu1\mu'|1M)V_{E1\mu',1^-\to1^+} + (\mu \longleftrightarrow \mu')$, where $V_{E1\mu,i\to f}$ is the μ-component of the interaction potential (for a spin-zero ground state, μ is also the angular momentum projection of the intermediate state). Assuming that the phases and the products of the reduced matrix elements for the two sequential excitations are equal, we obtain $V_{E1\mu,0\to1^-} \times V_{E1\mu',1^-\to1^+} = V_{E1\mu',0\to1^-} \times V_{E1\mu,1^-\to1^+}$. Thus, under these circumstances, and since $(001\mu|1\mu) \equiv 1$, we get an identically zero result for the excitation amplitude of the 1^+ DGDR state as a consequence of $(1\mu1\mu'|1M) = -(1\mu'1\mu|1M)$. A coupled-channels calculation cannot change this result appreciably.

We note that multiphonon states can be obtained by coupling all kinds of phonons. Each configuration $[\lambda_1^{\pi_1} \otimes \lambda_2^{\pi_2}]$ can be obtained theoretically from a sum over several two-
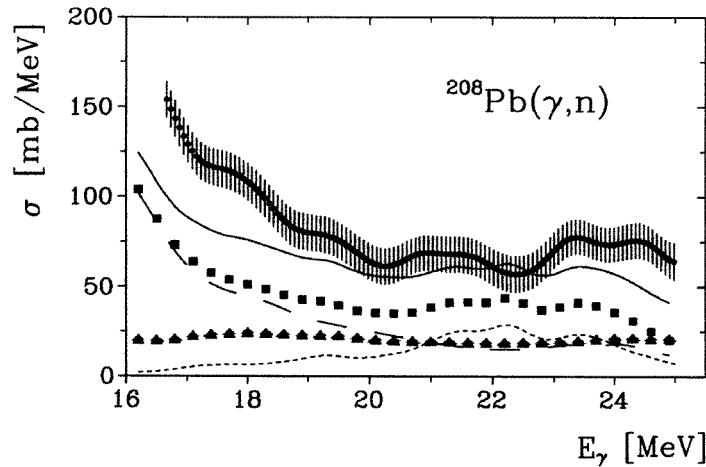
Figure 9. Photoneutron cross section for ^{208}Pb. Experimental data (dots with experimental errors) are from [28]. The long-broken curve is the high-energy tail of the GDR, the short-broken curve is the IVGQR and the curve with squares is their sum. The contribution of two-phonon states is plotted by a curve with triangles. The full curve is the total calculated cross section.
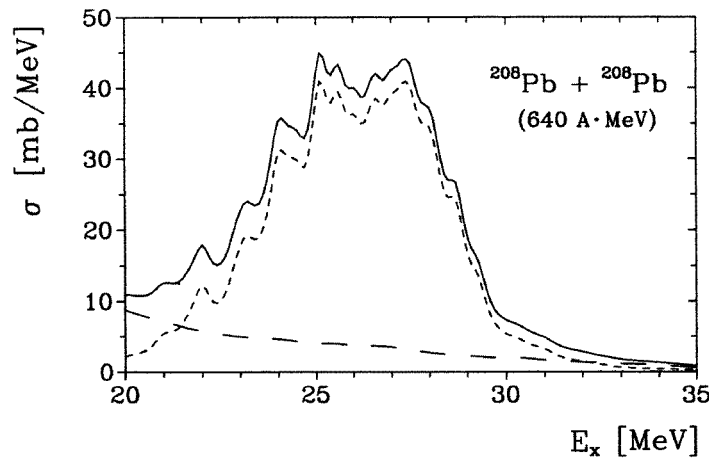

Figure 10. The contribution for the excitation of two-phonon 1^- states (long-broken curve) in first-order perturbation theory, and for two-phonon 0^+ and 2^+ DGDR states in second-order (short-broken curve). The total cross section (for ^{208}Pb($640A$ MeV) $+ \,^{208}$Pb) is shown by the full curve.

phonon states made of phonons with a given spin and parity $\lambda_1^{\pi_1}$, $\lambda_2^{\pi_2}$, and different RPA root numbers i_1, i_2 of its constituents. The cross sections can be obtained accordingly:

$$\sigma([\lambda_1^{\pi_1} \otimes \lambda_2^{\pi_2}]) = \sum_{i_1, i_2} \sigma([\lambda_1^{\pi_1}(i_1) \otimes \lambda_2^{\pi_2}(i_2)]). \tag{12}$$

As an example, in [27] the total number of two-phonon 1^- states generated in this way was about 10^5. The absolute value of the photoexcitation of any two-phonon state under consideration is negligibly small but altogether they produce a sizeable cross section. The 1^- two-phonon states obtained in [27] were used to calculate their contribution to the (γ, n)
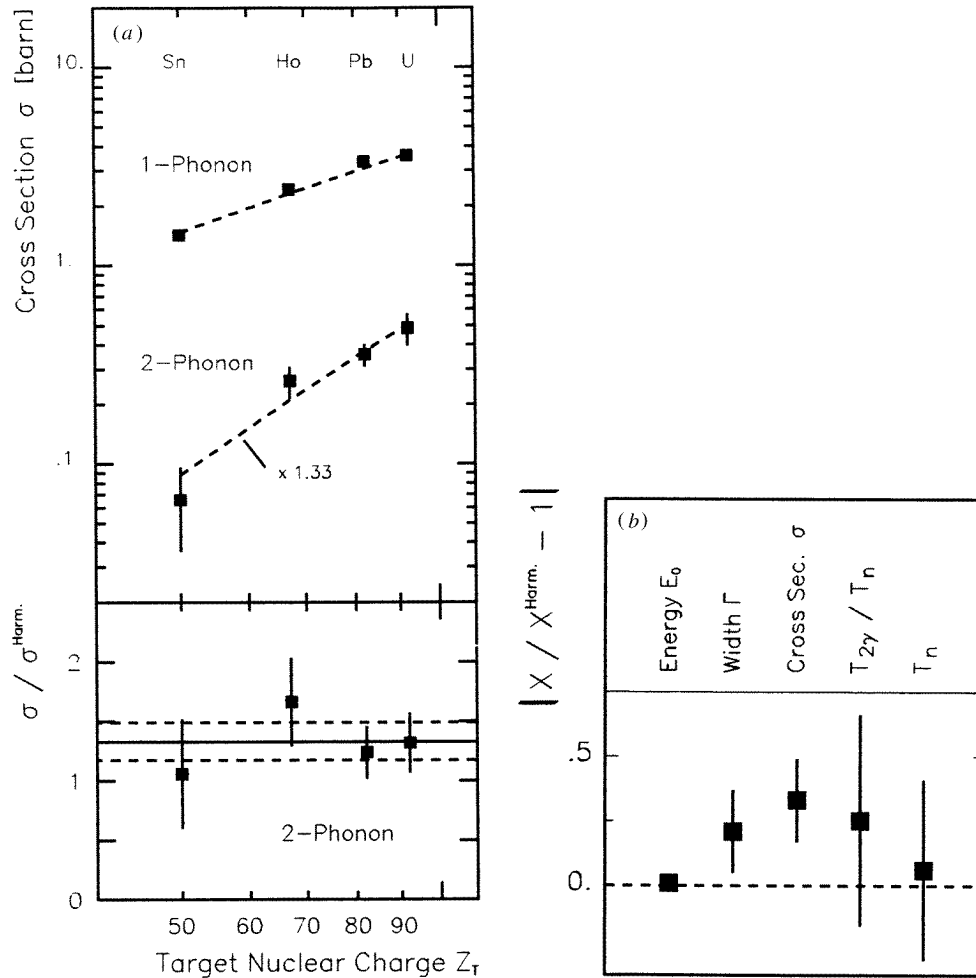
Figure 11. (*a*) Cross sections for the excitation of the GDR and of the DGDR in ^{208}Pb (640*A* MeV) incident on several targets. The ratio between the measured cross section and the prediction of the harmonic oscillator is also shown. (*b*) Deviation of the experimental results from the harmonic oscillator prediction for the energy, width, cross section, ratio between the decay by emission of two gammas, and of the one-neutron decay width, respectively.

cross section in ^{208}Pb, via direct $E1$ excitations. This is shown in figure 9. Experimental data (dots with experimental errors) are from [28]. The long-broken curve is the high-energy tail of the GDR, the short-broken curve is the IVGQR and the curve with squares is their sum. The contribution of two-phonon 1^- states is plotted by a curve with triangles. The full curve is the total calculated cross section. Thus, already at the level of photonuclear data the contribution of two-phonon 1^- states is of relevance. Here they are not reached via two-step processes, but in direct excitations. Since the energy region of these states overlap with that of the DGDR, in Coulomb excitation experiments they should also contribute appreciably. In fact, it was shown recently [27] that their contribution to the total cross section for ^{208}Pb + ^{208}Pb (640*A* MeV) in the DGDR region is of the order of 15%. In figure 10 the contribution for the excitation of two-phonon 1^- states (long-dashed curve) in

first order perturbation theory, and for two-phonon 0^+ and 2^+ DGDR states in second-order (short-dashed curve). The total cross section (for ^{208}Pb($640A$ MeV) $+$ ^{208}Pb) is shown by the solid curve.

2.5. *Present situation and perspectives*

The experimental situation on the excitation of double phonon states has improved considerably, mainly due to advances on the data acquisition with the Coulomb excitation technique. Figure 11(a) shows the comparison between the experimental cross section and the simple harmonic model (equations (2) and (3)) for the excitation of the GDR and the DGDR in ^{208}Pb ($640A$ MeV) and several targets [17]. One sees that the harmonic model reproduces the cross section for the GDR quite well, but it misses the magnitude of the cross section by 30%, as can be better seen in the lower part of the figure where the ratio between the experimental data and the calculation is shown. In figure 11(b) the present situation on the knowledge of the energy, width, excitation cross section, branching ratio for gamma to neutron emission, and the neutron emission width, respectively, is shown in comparison with calculations based on the simple harmonic picture. We see that the theory–experiment agreement is much better than that presented in figure 4.

As we have seen in this short review there are several effects which compete in the excitation of double giant resonances in relativistic Coulomb excitation. These effects were discovered in part by the motivation to explain discrepancies between the harmonic picture of the giant resonances and the recent experimental data. We cannot say at the moment by how much we have progressed towards a better understanding of these nuclear structures. However, we can surely say that the field is just at its infancy and important experimental and theoretical progress will be underway in the near future.

References

[1] Bothe W and Gentner W 1937 *Z. Phys.* **106** 236
[2] Goldhaber M and Teller E 1948 *Phys. Rev.* **74** 1046
[3] Steinwedel H and Jensen J H D 1950 *Z. Naturf.* **5a** 413
[4] Speth J and Wambach J 1991 *Int. Review of Nuclear and Particle Physics* vol 7, ed J Speth (Singapore: World Scientific)
[5] Emling H 1994 *Prog. Part. Nucl. Phys.* **33** 729
[6] Barrette J *et al* 1988 *Phys. Lett.* **209B** 182
[7] Beene J *et al* 1990 *Phys. Rev.* C **41** 920
[8] Beene J 1993 *Int. Nuclear Physics Conf. on Giant Resonances (Gull Lake)* (1994 *Nucl. Phys.* A **569** 163c)
[9] Baur G and Bertulani C A 1986 *Phys. Lett.* **174B** 23
    Baur G and Bertulani C A 1986 *Phys. Rev.* C **34** 1654
[10] Bertulani C A and Baur G 1988 *Phys. Rep.* **163** 299
[11] Bertulani C A and Nathan A M 1993 *Nucl. Phys.* A **554** 158
[12] Mordechai S *et al* 1988 *Phys. Rev. Lett.* **61** 531
[13] Schmidt R *et al* 1993 *Phys. Rev. Lett.* **70** 1767
[14] Ritman J L *et al* 1993 *Phys. Rev. Lett.* **70** 2659
[15] Vasconcellos-Gomes A C and Bertulani C A 1990 *Nucl. Phys.* A **517** 639
[16] Aumann T *et al* 1993 *Phys. Rev.* C **47** 1728

[17] Boretzky K *et al* 1996 *Phys. Lett.* B **384** 30
[18] Chomaz Ph and Frascaria N 1995 *Phys. Rep.* **252** 275
[19] Baur G and Bertulani C A 1996 *Proc. Int. School of Heavy Ion Physics (Erice, Italy, October 1986)* ed
     R A Broglia and G F Bertsch (New York: Plenum) p 331
[20] Bertulani C A and Zelevinsky V 1993 *Phys. Rev. Lett.* **71** 967
     Bertulani C A and Zelevinsky V 1993 *Nucl. Phys.* A **568** 931
[21] Canto L F, Romanelli A, Hussein M S and de Toledo Piza A F R 1994 *Phys. Rev. Lett.* **72** 2147
[22] Bertulani C A, Canto L F, Hussein M S and de Toledo Piza A F R 1996 *Phys. Rev.* C **53** 334
[23] Volpe C *et al* 1995 *Nucl. Phys.* A **589** 521
     Lanza E *et al* 1997 *Nucl. Phys.* A **613** 445
[24] Ponomarev V *et al* 1994 *Phys. Rev. Lett.* **72** 1168
     Ponomarev V *et al* 1996 *Z. Phys.* A **356** 251
[25] Bertsch G F and Feldmeier H 1997 *Phys. Rev.* C **56** 839
[26] Bertulani C A, Ponomarev V Yu and Voronov V V 1996 *Phys. Lett.* **388B** 457
[27] Ponomarev V and Bertulani C A 1997 *Phys. Rev. Lett.* **79** 3853
[28] Belyaev S N *et al* 1995 *Phys. At. Nucl.* **58** 1833